Vaspin Is an Adipokine Ameliorating ER Stress in Obesity as a Ligand for Cell-Surface GRP78/MTJ-1 Complex

Atsuko Nakatsuka,[1] Jun Wada,[1] Izumi Iseda,[1] Sanae Teshigawara,[1] Kanji Higashio,[3] Kazutoshi Murakami,[1] Motoko Kanzaki,[1] Kentaro Inoue,[1] Takahiro Terami,[1] Akihiro Katayama,[1] Kazuyuki Hida,[1] Jun Eguchi,[1] Chikage Sato Horiguchi,[2] Daisuke Ogawa,[2] Yasushi Matsuki,[4] Ryuji Hiramatsu,[4] Hideo Yagita,[5] Shigeru Kakuta,[6] Yoichiro Iwakura,[6,7] and Hirofumi Makino[1]

It is unknown whether adipokines derived from adipose tissues modulate endoplasmic reticulum (ER) stress induced in obesity. Here, we show that visceral adipose tissue–derived serine protease inhibitor (vaspin) binds to cell-surface 78-kDa glucose-regulated protein (GRP78), which is recruited from ER to plasma membrane under ER stress. Vaspin transgenic mice were protected from diet-induced obesity, glucose intolerance, and hepatic steatosis, while vaspin-deficient mice developed glucose intolerance associated with upregulation of ER stress markers. With tandem affinity tag purification using HepG2 cells, we identified GRP78 as an interacting molecule. The complex formation of vaspin, GRP78, and murine tumor cell DnaJ-like protein 1 (MTJ-1) (DnaJ homolog, subfamily C, member 1) on plasma membrane was confirmed by cell-surface labeling with biotin and immunoprecipitation in liver tissues and H-4-II-E-C3 cells. The addition of recombinant human vaspin in the cultured H-4-II-E-C3 cells also increased the phosphorylation of Akt and AMP-activated protein kinase (AMPK) in a dose-dependent manner, and anti-GRP78 antibodies completely abrogated the vaspin-induced upregulation of pAkt and pAMPK. Vaspin is a novel ligand for cell-surface GRP78/MTJ-1 complex, and its subsequent signals exert beneficial effects on ER stress–induced metabolic dysfunctions. ***Diabetes*** **61:2823–2832, 2012**

Obesity is associated with low-grade and chronic inflammation, which is a critical link between obesity and related metabolic dysfunction, such as insulin resistance and type 2 diabetes. Upstream of the obesity-induced inflammatory responses, endoplasmic reticulum (ER) stress and related signaling networks are emerging as a potential site for the interaction of inflammation and metabolic diseases (1). ER stress is induced by the accumulation of de novo synthesized unfolded proteins, and the unfolded protein response (UPR) is activated. The canonical UPR is linked to inflammatory and stress signal systems such as nuclear factor-κB (NF-κB)–IκB kinase, Jun NH_2-terminal kinase–activator protein 1 (AP1) pathways, and oxidative stress responses. Three major pathways of UPR, dsRNA-dependent protein kinase–like eukaryotic initiation factor 2α kinase (PERK)–mediated attenuation of translation, the activation of inositol requiring enzyme 1 (IRE1α) after splicing of mRNA of X-box binding protein 1 (XBP1), and activating transcription factor 6 (ATF6) pathway, have all been shown to be linked to inflammatory signaling (1). Causality between susceptibility to ER stress and insulin resistance has been shown to be supported by genetic manipulation of XBP1 (2) and ER chaperone proteins such as oxygen-regulated protein 150 (3,4) and 78-kDa glucose–regulated protein (GRP78) (5,6). In previous studies, XBP1 haploinsufficiency in mice resulted in insulin resistance (2) and oxygen-related protein 150 deficiency resulted in impaired glucose tolerance (3,4). Similarly, overexpression of GRP78 in the liver has been shown to result in beneficial metabolic effects in mice (6), and intriguingly, GRP78 heterozygosity has been shown to result in a compensatory increase in other ER chaperones, which enhanced overall ER capacity and consequently metabolic benefits (5).

We previously reported the cloning of visceral adipose tissue–derived serine proteinase inhibitor (vaspin), belonging to serpin clade A (*Serpina12*), and suggested that it may be a compensatory adipokine to improve insulin sensitivity with anti-inflammatory properties demonstrated by recombinant human vaspin protein (rhVaspin) administration into DIO mice (7,8). Since vaspin belongs to serpin, the identification of the proteases, which are inhibited by vaspin, may lead to the development of novel strategies in the treatment of obesity, diabetes, and insulin resistance; however, as of now molecular target(s) of vaspin and its mode of action are totally unknown (9). In later human studies, elevated serum vaspin concentrations in obesity (10), type 2 diabetes (11), and polycystic ovary syndrome (12) were reported, and it correlates with insulin resistance (homeostasis model assessment of insulin resistance) and C-reactive protein levels (13). Here, we show that vaspin exerts its compensatory actions on metabolic dysfunction associated with obesity by using genetic manipulation of the vaspin gene, i.e., in vaspin transgenic (Tg) and knockout mice. Further, we demonstrate that vaspin is a ligand for cell-surface–associated GRP78/MTJ-1 complex in the liver and provide a new functional insight into and molecular basis for the direct cross-talk between an adipokine and ER stress responses in obesity.

RESEARCH DESIGN AND METHODS

Generation of vaspin (*Serpina12*) Tg and knockout mice. β-Globin intron and human GH poly A signal were ligated into *BamH*I-*EcoR*I and *EcoR*I-*Xho*I sites of pcDNA3.1Zeo vector (Invitrogen), respectively. Coding region of

From the [1]Department of Medicine and Clinical Science, Okayama University Graduate School of Medicine, Dentistry and Pharmaceutical Sciences, Okayama, Japan; the [2]Department of Diabetic Nephropathy, Okayama University Graduate School of Medicine, Dentistry and Pharmaceutical Sciences, Okayama, Japan; [3]Metabolome Pharmaceuticals, Inc., Tokyo, Japan; [4]Genomic Science Laboratories, Dainippon Sumitomo Pharma, Osaka, Japan; the [5]Department of Immunology, Juntendo University School of Medicine, Tokyo, Japan; the [6]Center for Experimental Medicine and Systems Biology, The Institute of Medical Science, The University of Tokyo, Tokyo, Japan; and [7]Core Research for Evolutional Science and Technology, Japan Science and Technology, Saitama, Japan.

Corresponding author: Jun Wada, junwada@md.okayama-u.ac.jp.

Received 23 February 2012 and accepted 26 May 2012.

DOI: 10.2337/db12-0232

This article contains Supplementary Data online at http://diabetes.diabetesjournals.org/lookup/suppl/doi:10.2337/db12-0232/-/DC1.

mouse vaspin (*Serpina12*) cDNA was inserted into the *EcoR*I site by blunt end ligation after filling-in reaction. *BamH*I and *Xho*I fragment was subjected to blunt end ligation into *Sma*I site of pBluescript SKII(+) (Stratagene), in which mouse aP2 promoter was inserted into *EcoRV-Pst*I site by blunt end ligation (14). The insert was excised with *Hind*III and *Not*I, and transgene was generated. Microinjected C57BL/6JJcl one-cell stage zygotes were oviduct transferred and permitted to develop to term. Three Tg founders were obtained, and Southern blot analysis was performed using *Apa*I fragment of the transgene. Genotyping of Tg mice was performed by PCR using primers 5′-CAAGCTACTGCAGAGGCTGGCCAGCAATAG-3′ and 5′-GAGAGCTGGCTGTCATAGGCCATGTCGTAC-3′.

We also constructed a targeting vector for vaspin (*Serpina12*) using pBI-lx-Neo-DT carrying neomycin-resistance gene (*Neo*) to target exon 2 (Supplementary Fig. 7*A*) (15). The 5′ and 3′ homology arms were amplified from mouse genomic DNA using TaKaRa Ex Taq. The following primer pairs were used to amplify the homology arms: 5′-GGATCTGAGGGAAGCTGAGG-3′ and 5′-CCCATCTTAGCCATCATCAGGAG-3′ (for the 5′ homology arm) and 5′-GCTAGTCCATCTAGACAATCCG-3′ and 5′-CCAGCATAGTCGTGAGGATG-3′ (for the 3′ homology arm). Homologous recombination of 129P2/OlaHsd embryonic stem cell clones was screened by Southern blot using *BamH*I-digested genomic DNA with a 3′-probe. Recombination was further confirmed by *Mun*I-digested DNA with a 5′-probe and *Sca*I-*Cla*I–digested DNA with a Neo-probe (Supplementary Fig. **7***A*). Male chimeric mice were mated with C57BL/6JJcl mice to generate heterozygous vaspin$^{+/-}$ mice, and they were backcrossed to C57BL/6JJcl mice for more than five generations. Genotyping of vaspin$^{-/-}$ mice was performed by PCR using primers 5′-CCGACTCGAGATAACTTCGT-3′ and 5′-CTGGAAGGCAAGGACTGACTG-3′, and vaspin$^{+/+}$ mice were identified by 5′-GAGGACCTGAGTTCAGACTCC-3′ and CACCGTCCACCAGATTCAGG-3′.

Animals. Male mice were housed in cages and maintained on a 12-h light-dark cycle. For the animal experiments with mice, standard chow (NMF; Oriental Yeast) and a high fat–high sucrose (HFHS) diet (D12331; Research Diet) were used and the mice were killed at 25 weeks of age. Oxygen consumption was measured using an O_2/CO_2 metabolism–measuring system (MK-5000; Muromachi). Ambion In Vivo small interference (si)RNA Predesigned siRNA (HPLC In Vivo Ready) was injected into vaspin Tg and wild-type (WT) HFHS diet–fed mice at a dose of 7 mg/kg following the protocol supplied with Invivofectamine 2.0 Reagent (Invitrogen). All animal procedures were performed in accordance with the Guide for Care and Use of Laboratory Animals at the Department of Animal Resources, Advanced Science Research Center, Okayama University. Liver triglyceride was measured by Folch method (Skylight Biotech, Tokyo, Japan).

Cell culture. H-4-II-E-C3 cells (European Collection of Cell Cultures) were cultured in minimum essential medium Eagle containing 2 mmol/L glutamine, 1% nonessential amino acids, and 10% FBS. HepG2 cells (American Type Culture Collection) were cultured in minimum essential medium Eagle containing 2 mmol/L glutamine, 1 mmol/L sodium pyruvate, 1% nonessential amino acids, and 10% FBS. H-4-II-E-C3 cells were transfected with 5 multiplicity of infection of MISSION short-hairpin (sh)RNA lentivirus transduction particles for GRP78 (GenBank accession number NM_022310) and nontarget shRNA control lentivirus transduction particles, and they were further treated with various concentrations of rhVaspin.

Poly(A$^+$) RNA analysis. For quantitative real-time PCR analysis, cDNA synthesized from 2 μg of total RNA was analyzed in a sequence detector (model 7900; PE Applied Biosystems) with specific primers and SYBR Green PCR Master (PerkinElmer Life Sciences). The relative abundance of mRNAs was standardized with 36B4 mRNA as the invariant control. The mRNA expression was determined by SYBR green. Gene-specific primers are indicated in Supplementary Table 1.

Western blot analysis. Mice were starved overnight, anesthetized with pentobarbital and injected with 5 units of regular human insulin into the inferior vena cava, and liver was removed 5 min after the injection. Liver tissues were fractionated by discontinuous iodixanol gradients following protocol S36 of the manufacturer's application sheets (OptiPrep; Invitrogen). The protein lysates of total and subcellular fractions of liver tissues as well as H-4-II-E-C3 were subjected to SDS-PAGE and transferred to polyvinylidene fluoride membranes. The membranes were treated with specific antibodies (1:200–1,000 dilution): GRP78 (C-20), PGC-1 (H-300), Na^+/K^+-ATPase α1 (*N*-15), and vaspin (I-14) (Santa Cruz); vaspin (Strategic Biosolutions); phospho-Akt (Ser473), Akt, phospho–AMP-activated protein kinase (AMPK)α (40H9), SirT1 (C14H4), phospho-eIF2α (Ser51), and GAPDH (14C10) (Cell Signaling); calnexin (ab22595) and IRE1α (phospho-S724) (Abcam); and Golgi 58 K (58K-9) and DNAJC1 (Sigma) overnight at 4°C. Antibody treatment was followed by treatment with secondary antibodies conjugated with horseradish peroxidase and, finally, visualization with ECL Plus (GE Healthcare) and a luminescent image analyzer (LAS-3000mini; Fujifilm). Immunoprecipitation was performed using Universal Magnetic Co-IP kit (Active Motif). Cell-surface proteins of H-4-II-E-C3 were biotinylated and isolated using Pierce Cell Surface Protein Isolation kit.

Liquid chromatography–tandem mass spectrometry. Recombinant full-length mouse vaspin (vaspin-Ad) and vaspin tagged with calmodulin and streptavidin-binding peptides (pCTAP-vaspin-Ad) (InterPlay Mammalian TAP system; Stratagene) were prepared by Adenovirus Expression Kit (Takara) as previously described (8). Adenovirus vector–expressing vaspin tagged with calmodulin and streptavidin-binding peptides (pCTAP-vaspin-Ad) was introduced to HepG2. Soluble proteins were purified by CBP- and SBP-binding resin (InterPlay Mammalian TAP System; Stratagene) and subjected to SDS-PAGE and Coomassie Blue staining. Visible bands were excised and in-gel digested with trypsin and analyzed with liquid chromatography–tandem mass spectrometry (LC-MS/MS) (16).

Pull-down assay and ^{125}I-vaspin binding analysis. Coding sequences without signal peptide of vaspin$^{21–413}$ and GRP78$^{19–654}$ were ligated to *Kpn*I-*Xba*I and *Sal*I-*Not*I sites of pTNT vector (Promega), respectively. Coding sequence without signal peptide of vaspin$^{21–413}$ was ligated to *BamH*I-*Xho*I site, GRP78 to *Sal*I-*Not*I and α1-antitrypsin (α1AT)$^{26–417}$, and chimeric vaspin$^{21–249}$/α1AT$^{254–417}$ and α1AT$^{26–253}$/vaspin$^{250–413}$ to *EcoR*I - *Not*I of pET-42a vector. Pull-down assay was performed with MagneGST Pull-Down System (Promega). rhVaspin was iodinated with specific activity of 7.8 μCi/μg (PerkinElmer) and used for solid-phase assay. Cell-binding assay of cultured H-4-II-E-C3 was performed using ^{125}I-vaspin and subjected to Scatchard analysis. Liver membrane fractions were isolated, and the binding activity of ^{125}I-vaspin was also investigated (9). α2-macrogloburin (α2M) (Abnova), anti-GRP78 (*N*-20), and anti-GRP78 (C-20) were used for the pull-down and solid-phase binding assays.

Statistical analysis. Data are expressed as means ± SEM and analyzed by unpaired Student *t* test in the comparison of two groups and two-way ANOVA in the comparison of more than three groups. Oxygen consumption was compared by ANCOVA with body weight as a covariant. $P < 0.05$ was regarded as statistically significant. The data were analyzed with PASW Statistics 18 (SPSS, Chicago, IL).

RESULTS

Vaspin improves insulin sensitivity in vivo. Vaspin Tg C57BL/6JJcl mice under the control of aP2 promoter were produced (Supplementary Fig. 1*A*), and the vaspin levels in serum and adipose tissues derived from three independent lines (line 1, line 10, and line 58) were comparable, although copy numbers of transgene were different in the three lines (Supplementary Fig. 1*B–D*). At 25 weeks of age, the body weight gain was ameliorated by ~8% (Fig. 1*A*) and fat pad and liver weight were significantly reduced (Fig. 1*B*) in Tg mice of line 1 compared with WT mice. Mice fed with HFHS chow demonstrated similar weight reduction in all three lines (Supplementary Fig. 1*E*), and the representative data of line 1 are shown. Although the pathological features of steatohepatitis such as infiltration of inflammatory cells were not observed in either vaspin Tg or WT mice, by Oil Red O staining, the lipid droplets in the liver were apparently reduced (Fig. 1*C*), and triglyceride content was also significantly decreased in HFHS chow Tg mice, suggesting that liver may be one of the major target organs of vaspin. In the sera, leptin and insulin levels were significantly reduced at 13 weeks of age in HFHS chow mice, but there were no differences at 25 weeks of age (Supplementary Fig. 2*A–C*). The results suggested that vaspin may not completely compensate for insulin resistance associated overall with obesity and aging. In addition, vaspin overexpression did not alter the serum concentration of adiponectin (Supplementary Fig. 2*D*). Gel filtration HPLC indicated a small reduction in the fraction of small dense LDL cholesterol (Supplementary Fig. 2*E–G*). Glucose tolerance and insulin tolerance tests demonstrated improvement of insulin sensitivity in Tg mice (Fig. 1*D* and *E* and Supplementary Fig. 3*A* and *B*). In the liver tissues, real-time PCR demonstrated the reduction of gluconeogenic genes *G6pc* and *Pepck* and lipogenesis genes *Acc*, *Fasn*, and *Scd1* (Supplementary Fig. 4*A–H*). In proinflammatory cytokines, serum interleukin-6 levels were significantly reduced in

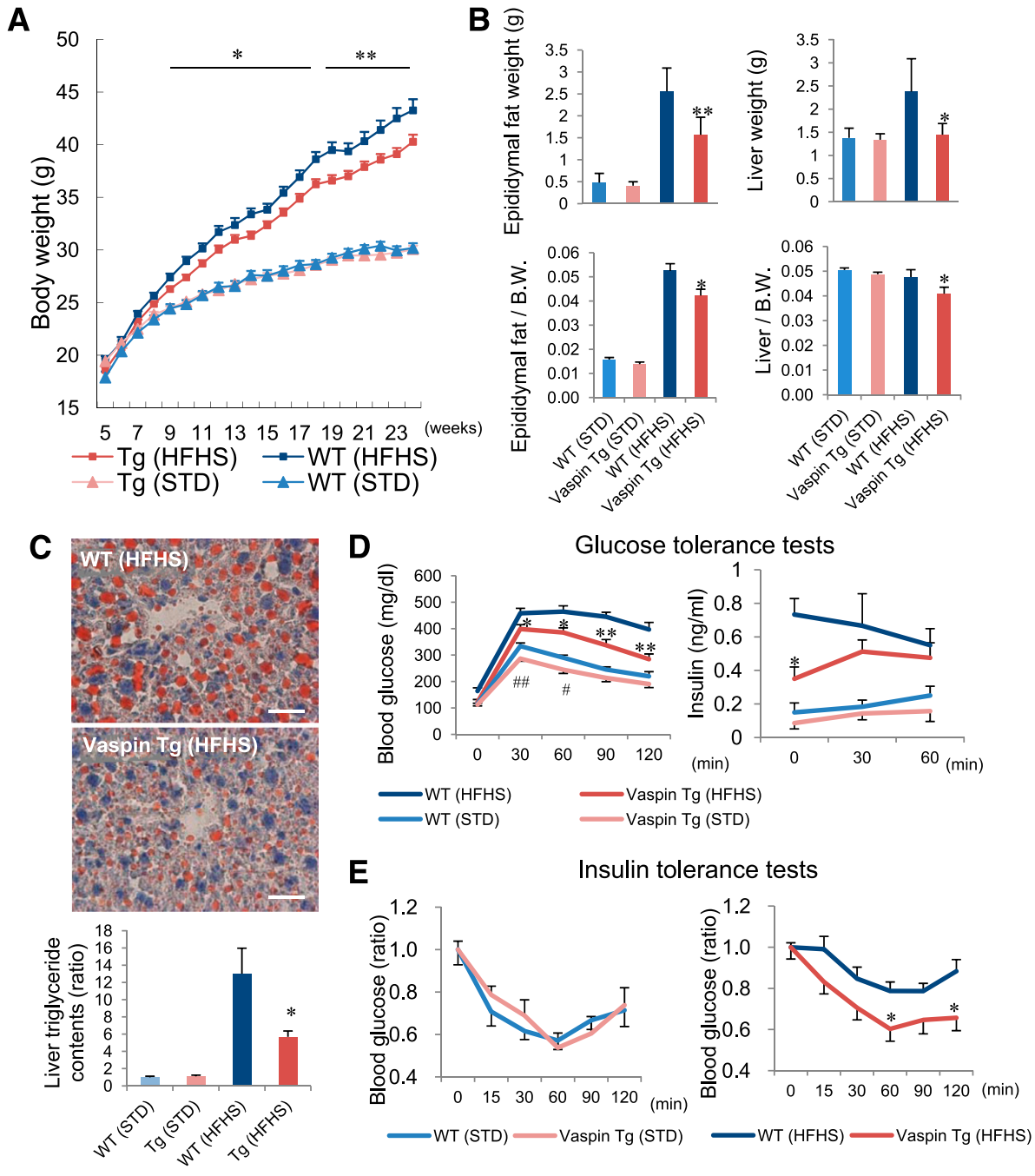

FIG. 1. Phenotype of WT and vaspin Tg mice. *A*: Body weight of WT and vaspin Tg mice fed standard (STD) and HFHS chow (n = 20). *B*: Epididymal fat and liver weight of WT and vaspin Tg mice at 25 weeks of age (n = 5–9). B.W., body weight. *C*: Oil Red O staining of liver and triglyceride contents of WT and vaspin Tg mice at 25 weeks of age. Triglyceride contents were normalized by liver weight, and fold changes compared with WT normal chow mice are indicated. Bar = 300 μm (n = 5–9). *D*: Glucose tolerance test at 12 weeks of age (1.5 mg/kg body wt i.p.) (n = 5–9). *E*: Insulin tolerance test at 12 weeks of age (0.75 units/kg body wt i.p. for standard chow and 1.0 units/kg body wt i.p. for HFHS) (n = 4–10). All values are presented as means ± SEM. *P < 0.05, **P < 0.01 vs. WT HFHS mice; #P < 0.05, ##P < 0.01 vs. WT HFHS mice. (A high-quality digital representation of this figure is available in the online issue.)

vaspin Tg HFHS chow mice (Supplementary Fig. 4*I*–*K*). To survey the gene expression profile in adipose tissues, we further evaluated the expression of 22,626 genes by Mouse Gene 1.0 ST Array (Affymetrix). Among 22,626 genes, 350 genes and 26 immune response genes revealed significant variation across the samples. Hierarchical clustering analysis of these genes revealed that mesenteric gene expression profile in vaspin Tg mice fed with high-fat chow was on same branch as in mice fed with normal chow, suggesting that the expression pattern of immune response genes became close to that of control mice fed with normal chow (Supplementary Fig. 5*A* and *B*). Food intake and locomotor activities were unaltered (Supplementary Fig. 6*A*–*C*), and VO_2 did not changed in vaspin Tg HFHS diet–fed mice with ANCOVA with body weight as a covariate (Supplementary Fig. 6*D*). The hypertrophy of adipocytes was ameliorated and the crown-like structures were also reduced in Tg HFHS chow mice (Supplementary Fig. 6*E*).

For further confirmation of the phenotype of Tg mice, the standard gene-targeting method was used to produce vaspin knockout mice (Supplementary Fig. 7*A*). Elevation of mRNA and protein expression of vaspin in the epididymal adipose tissues and serum was observed in vaspin$^{+/+}$ HFHS chow mice; however, it was not observed in vaspin$^{-/-}$ mice (Supplementary Fig. 7*B*). Vaspin$^{-/-}$ HFHS diet–fed mice demonstrated increase in body weight, fat pad, and liver weight (Fig. 2*A* and *B*). The size of adipocytes and the number of crown-like structures increased in vaspin$^{-/-}$ mice (Fig. 2*C* and Supplementary Fig. 6*F*), and deterioration of insulin sensitivity was observed (Fig. 2*D* and *E* and Supplementary Fig. 3*C* and *D*). Serum total cholesterol and small dense LDL cholesterol levels were significantly increased in vaspin$^{-/-}$ mice (Supplementary Fig. 8*A*–*C*). Serum leptin levels increased at 25 weeks of

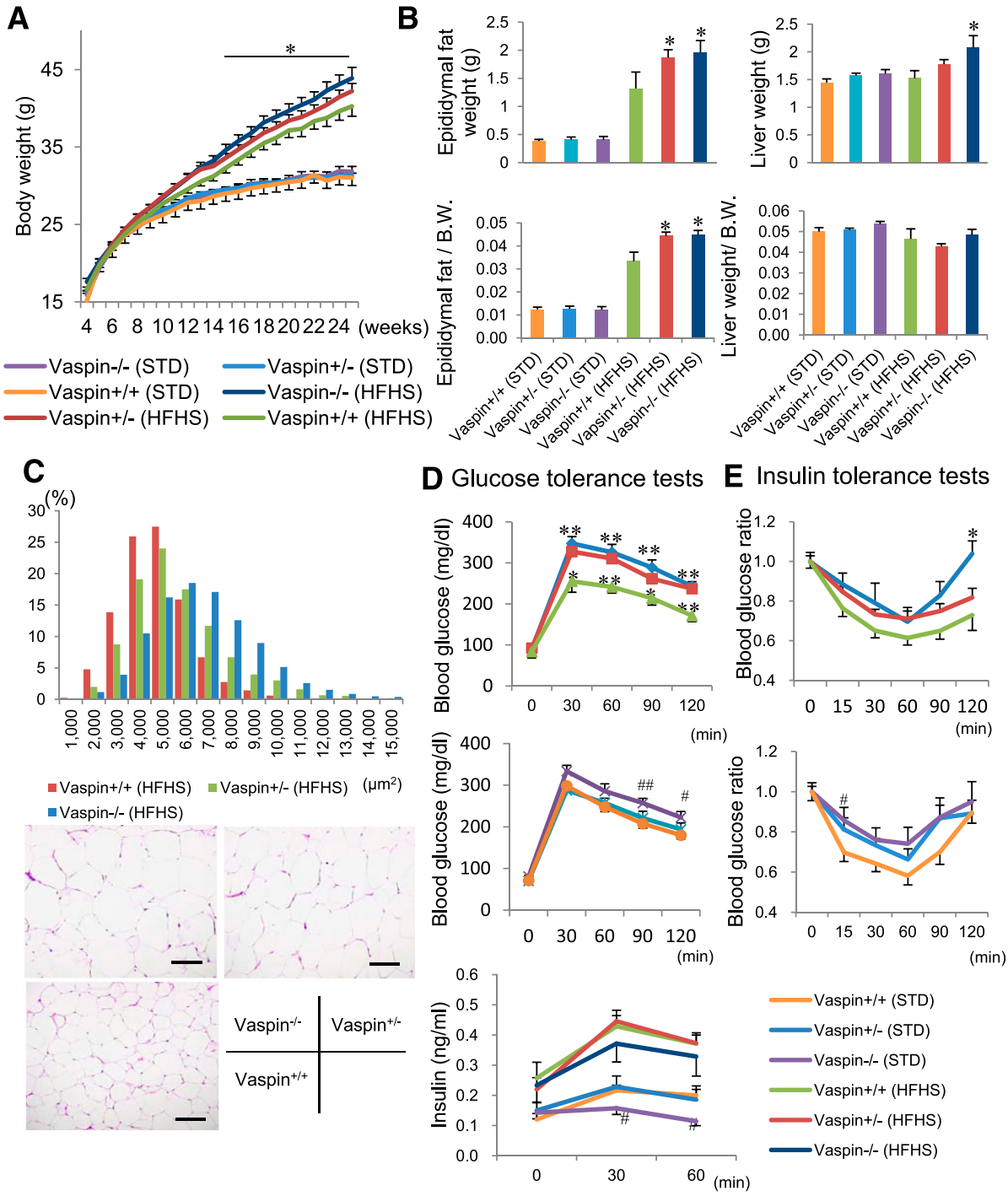

FIG. 2. Phenotype of vaspin$^{+/+}$, vaspin$^{+/-}$, and vaspin$^{-/-}$ mice. *A*: Body weight of vaspin$^{+/+}$, vaspin$^{+/-}$, and vaspin$^{-/-}$ fed standard (STD) and HFHS chow (n = 20). *B*: Epididymal fat and liver weight of vaspin$^{+/+}$, vaspin$^{+/-}$, and vaspin$^{-/-}$ mice at 25 weeks of age (n = 8–12). B.W., body weight. *C*: The adipocyte size of epididymal fat pad and histological appearance in periodic acid Schiff staining (bar = 100 μm) (n = 5). *D*: Glucose tolerance test at 12 weeks of age (1.5 mg/kg body wt i.p.). *E*: Insulin tolerance test at 12 weeks of age (0.75 units/kg body wt i.p. for standard chow and 1.0 units/kg body wt i.p. for HFHS) (n = 5–7). Values are presented as means ± SEM in *A*–*E*. *P < 0.05, **P < 0.01 vs. vaspin$^{+/+}$ HFHS mice; #P < 0.05, ##P < 0.01 vs. vaspin$^{+/+}$ HFHS mice. (A high-quality digital representation of this figure is available in the online issue.)

age and, in accordance with the results in vaspin Tg mice, serum concentration of adiponectin was not altered in vaspin$^{-/-}$ mice, suggesting that the vaspin-mediated improvement of insulin tolerance is not dependent on the adiponectin pathway (Supplementary Fig. 8*D* and *E*). Triglyceride contents prominently increased in vaspin$^{-/-}$ and vaspin$^{+/-}$ HFHS chow mice compared with vaspin$^{+/+}$ mice (Supplementary Fig. 8*F* and *G*). The impact of gene manipulation of vaspin on the body and fat pad weight was rather less impressive compared with the changes in insulin sensitivities and triglyceride contents in the liver. We thus speculated that secreted vaspin from visceral adipose tissue may exert such effects directly acting on liver cells and further investigated to identify the vaspin-interacting molecules in the liver.

Vaspin interacts with GRP78. Serpin clade A members consist of classical serine proteases inhibitors, such as antitrypsin (*SERPINA1*) and antichymotrypsin *(SERPINA3*), hormone-binding proteins (*SERPINA6*, corticosteroid-binding globulin; *SERPINA7*, thyroxine-binding globulin), and angiotensinogen (*SERPINA8*). The diverse function of serpin clade A members led us to further screen and search for the molecules interacting with vaspin. We failed to demonstrate that vaspin inhibits the activities of known serine proteases. Vaspin failed to bind to cortisol and thyroxine, and vaspin did not alter the protease cascades in renin angiotensin and complement systems. We further screened the interacting molecules by tandem affinity tag purification. pCTAP-vaspin-Ad was applied to HepG2 cells, purified by calmodulin and streptavidin resin, subjected to SDS-PAGE and in-gel digestion with trypsin, and analyzed by LC-MS/MS, and we identified GRP78 as an interacting molecule in HepG2 cells. Since GRP78 was not isolated in the nontransfected cell lysates, GRP78 specifically bound to vaspin but not to calmodulin and streptavidin resin (Fig. 3*A*). Immunoprecipitation study indicated the presence of vaspin-GRP78 complex in HepG2 cells supplemented with rhVaspin in the culture media, and it was not found in HepG2 cells, in which vaspin was not expressed (Fig. 3*B*). Pull-down assay demonstrated the physical binding between in vitro–translated GRP78 and glutathione S-transferase (GST)-vaspin recombinant proteins (Fig. 3*C*) as well as between GST-GRP78 and in vitro–translated vaspin proteins (Fig. 3*D*). By pull-down assay, GST-vaspin$^{21–249}$/α1AT$^{254–417}$ bound to GRP78 but GST-α1AT$^{26–253}$/vaspin$^{250–413}$ failed to bind GRP78, suggesting that GRP78 bound to the NH_2-terminal half of vaspin, avoiding the reactive site loop at COOH-terminal, which is a conserved domain of serpin (Supplementary Fig. 9*A*). In pull-down assays, the binding between GST-vaspin and GRP78 was inhibited by the addition of anti-GRP78 (C-20) (Supplementary Fig. 9*B*), and the binding between immobilized GRP78 and vaspin in solid-phase binding assay was inhibited by both anti-GRP78 (*N*-20) and anti-GRP78 (C-20) at the concentration of 40 μg/mL (Supplementary Fig. 9*C*). GRP78 has NH_2-terminal nucleotide-binding domain, a compact β-sandwich domain harboring a cleft for substrate binding and a lid domain with α-helical structure at COOH-terminal end (17). Anti-GRP78 (*N*-20) and anti-GRP78 (C-20) were raised against ATP-binding domain and COOH-terminal lid domain, respectively. Thus, the binding between vaspin and GRP78 is disrupted by interference of the conformation of ATP-binding and COOH-terminal lid domains. We also demonstrated the colocalization of vaspin and GRP78 in HepG2 cells that were transfected with adenovirus expressing full-length of mouse vaspin (vaspin-Ad) by double immunostaining methods (Supplementary Fig. 10).

Vaspin is a ligand for plasma membrane–associated GRP78. We investigated the expression of known GRP78-associated anchor proteins, MTJ-1, ATF6, IRE1α, and PERK, in the liver. We performed Western blot analysis using cell fractions of liver tissues of Tg and WT mice. We demonstrated the expression of MTJ-1 in the plasma membrane fractions of the livers from HFHS chow–fed mice (Supplementary Fig. 11). The biotinylated cell-surface proteins in H-4-II-E-C3 cells were isolated by NeutrAvidin agarose resin, and Western blot analysis revealed that vaspin, GRP78, and MTJ-1 coexisted as cell-surface proteins (Supplementary Fig. 11*E*). Furthermore, through use of the plasma membrane fractions of the liver, vaspin coprecipitated with GRP78 and MTJ-1 (Supplementary Fig. 11*F*) and GRP78 coprecipitated with MTJ-1 in both vaspin Tg and WT mice (Supplementary Fig. 11*G*), suggesting that they formed a complex in the plasma membrane fractions. α2M is a known ligand for GRP78/MTJ-1, which induces phosphorylation of Akt. In pull-down and solid-phase binding assays, α2M did not efficiently compete with the binding between vaspin and GRP78 (Supplementary Fig. 12*A* and *B*); however, vaspin and α2M were colocalized in the sinusoidal front of liver cells in vaspin Tg mice (Supplementary Fig. 12*C*). Since α2M is abundant in serum (~100 mg/dL) and serum vaspin levels have been reported to be ~1–10 ng/mL, the binding affinity of vaspin is quite high compared with α2M and excess amount of α2M is required to compete with vaspin.

Phosphorylation of Akt was enhanced in Tg and suppressed in vaspin$^{-/-}$ mice treated with HFHS diet (Fig. 4*A*). Similarly, phosphorylation of AMPK was markedly enhanced in Tg mice and suppressed in vaspin$^{-/-}$ mice without alterations in the expression of Sirt1 or peroxisome proliferator–activated receptor γ coactivator 1α (Fig. 4*A* and Supplementary Fig. 13). The addition of rhVaspin in the culture also increased the phosphorylation of Akt and AMPK in H-4-II-E-C3 in a dose-dependent manner (Fig. 4*B*). The application of anti-GRP78 (*N*-20) and anti-GRP78 (C-20) completely abrogated the vaspin-induced phosphorylation of Akt (Fig. 4*C*). The activation of pAMPK was also efficiently repressed by anti-GRP78 (*N*-20) and anti-GRP78 (C-20) (Fig. 4*C*). Although the vaspin-binding site on GRP78 is still unknown, the data suggested that ATP domain at NH_2-terminal and highly helicated COOH-terminal lid domain of GRP78 are important for the vaspin-induced intracellular signaling. Since GRP78 was recruited from ER to plasma membrane fractions under ER stress, we also investigated the ER stress–related markers in vaspin Tg and vaspin$^{-/-}$ HFHS mice. Among ER stress–related factors, upregulation of ATF6, pelF2α, and pIRE1α by HFHS treatments was ameliorated in vaspin Tg mice; in contrast, they were upregulated in vaspin$^{-/-}$ HFHS mice compared with vaspin$^{+/+}$ mice (Supplementary Fig. 13).

To further confirm that vaspin is an authentic ligand for cell-surface GRP78 complex, we performed the knockdown experiments in vaspin Tg mice and H-4-II-E-C3 cells. The expression of GRP78 was reduced by ~40% by the treatment of in vivo–injected siRNA-GRP78 (Fig. 5*A*). Glucose tolerance tests revealed that siRNA-GRP78 treatment deteriorated glucose tolerance in both vaspin Tg and WT mice, and the insulin-sensitizing action of overexpressed vaspin disappeared in vaspin Tg mice (Fig. 5*B* and *C*). Binding assay using ^{125}I-vaspin in isolated membrane fractions of the liver and H-4-II-E-C3 cells revealed

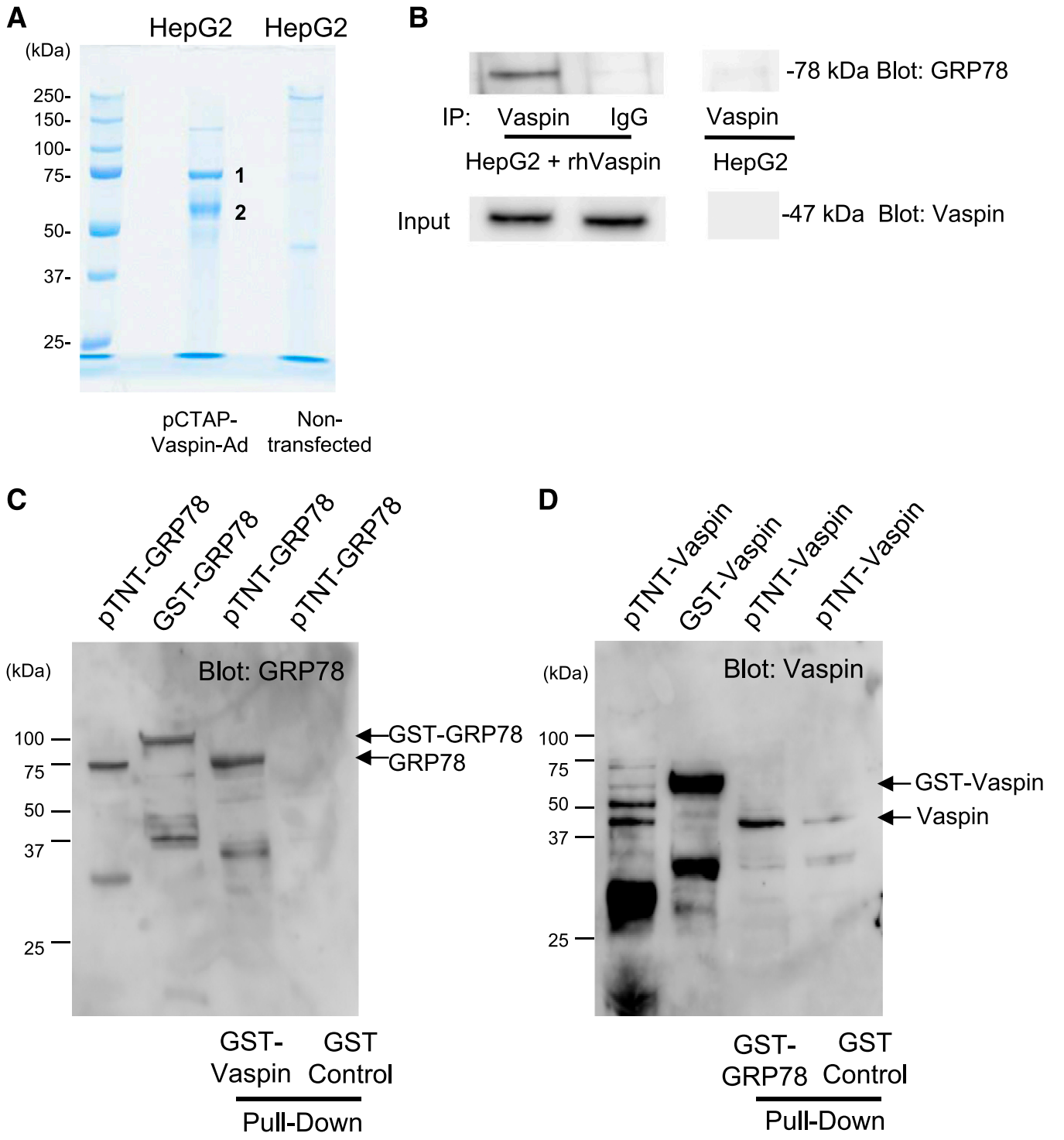

FIG. 3. Identification of GRP78 and vaspin complex by tandem affinity tag purification. *A*: pCTAP-vaspin-Ad was applied to HepG2, and purified products were analyzed by SDS-PAGE. In-gel digestion with trypsin and analysis by LC-MS/MS revealed that band 1 is GRP78 and band 2 is vaspin. *B*: HepG2 was treated with vaspin recombinant protein. Vaspin-GRP78 complex was immunoprecipitated by vaspin antibody and blotted with GRP78 antibodies. *C*: Pull-down assay using GST-vaspin fusion protein and in vitro–translated GRP78. *D*: Pull-down assay using GST-GRP78 fusion protein and in vitro–translated vaspin. (A high-quality color representation of this figure is available in the online issue.)

high-affinity binding with K_d values 22.2×10^{-9} and 0.57×10^{-9} mol/L, respectively. The treatments of siRNA-GRP78 and shRNA-GRP78 lentivirus did not alter the binding affinity (24.0×10^{-9} and 0.53×10^{-9} mol/L in liver and H-4-II-E-C3 cells, respectively); however, they reduced B_{max} both in vivo and in vitro (Fig. 5*D* and *E*).

DISCUSSION

GRP78 is an ER chaperone that binds to hydrophobic patches of nascent polypeptides in ER and serves as a switch for the induction of UPR. GRP78 directly binds to IRE1α, ATF6, and PERK under normal conditions. Under ER stress, the available pool of GRP78 is occupied by

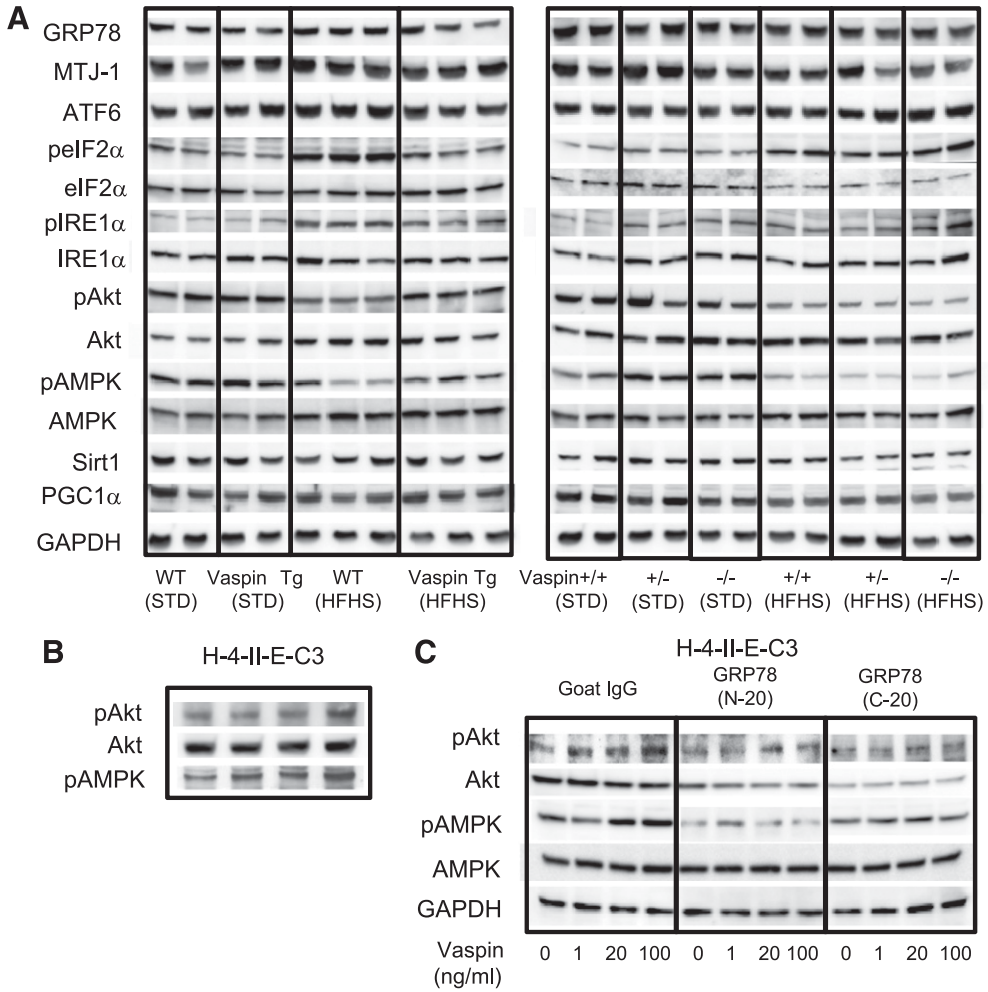

FIG. 4. Western blot analyses of liver and cultured cells. *A*: Western blot analyses of the livers from WT, vaspin Tg, vaspin$^{+/+}$, vaspin$^{+/-}$, and vaspin$^{-/-}$ mice fed standard (STD) and HFHS chow. Upregulation of pAkt and pAMPK was noted in vaspin Tg mice, and pAkt and pAMPK were downregulated in vaspin$^{-/-}$ HFHS mice. ATF6, peIF2α, and pIRE1α were upregulated in vaspin$^{-/-}$ HFHS mice. *B*: In H-4-II-E-C3 cells, pAkt and pAMPK were enhanced by treatment of rhVaspin. *C*: Non-target shRNA control lentivirus transduction particles upregulated basal activity of pAkt; however, treatment of shRNA lentivirus for MTJ-1 and GRP78 suppressed pAkt in H-4-II-E-C3 cells. Impact on pAMPK was minimal by the treatment of shRNA lentivirus for MTJ-1 and GRP78. GAPDH, glyceraldehyde-3-phosphate dehydrogenase.

preventing the aggregation of unfolded proteins, and GRP78 releases IRE1α, ATF6, and PERK, which are transducers of the UPR signals (1). Beyond the ER retention, GRP78 is also associated with various anchor membrane proteins on the cell surface and functions as a receptor for various ligands and a signaling hub for cell survival or death (18–21). In many tumor cells, α2M binds to cell-surface GRP78/MTJ-1, activates phosphatidylinositol 3-kinase/Akt signal to suppress apoptotic pathways, concomitantly upregulates NF-κB, and induces UPR so that cell proliferation occurs (22–25). In addition to α2M, teratocarcinoma-derived growth factor-I (Cripto) and GRP78 form a complex at the cell surface and enhance the cell growth by inhibiting transforming growth factor-β signaling events (26). Truncated cadherin and GRP78 exert the activation of Akt and promote the survival of vascular endothelial cells (27). In obesity associated with metabolic dysfunction, plasmalemmar GRP78/MTJ-1 is induced in the liver, and the association of vaspin and GRP78/MTJ-1 transduces the intracellular signaling such as activation of Akt and AMPK, which results in the improvement of both glucose and lipid metabolism. The activation of Akt and AMPK was demonstrated in the liver of vaspin Tg mice, the downregulation was observed in vaspin$^{-/-}$ HFHS diet–fed mice, and the activation of Akt and AMPK signaling was also confirmed in cultured H-4-II-E-C3 cells. In addition, major ER stress pathways such as ATF6, peIF2α, and pIRE1α were enhanced in vaspin$^{-/-}$ HFHS mice. Thus, vaspin modulates the ER stress responses through outside-in signal via cell-surface GRP78, and it has beneficial effects on multiple organs by ameliorating the metabolic dysfunction and inflammatory responses in obesity. Energy expenditure, oxygen consumption, was not significantly altered in vaspin Tg or vaspin$^{-/-}$ mice HFHS mice; however, a reduction of body weight in vaspin Tg HFHS mice and an increase in body weight in vaspin$^{-/-}$ HFHS mice were observed. One can speculated that the methods of measuring food intake and energy expenditure are not sensitive enough to detect differences or that food absorption may be altered in vaspin Tg and in vaspin$^{-/-}$ mice. We demonstrated the alteration of ER stress molecules in the current investigation; we can speculate that vaspin may alter the ER stress primarily as opposed to vaspin directly regulating energy expenditure.

Targeting GRP78 for therapeutics against obesity, autoimmune diseases, and cancers has been postulated (1,18). In obesity with metabolic dysfunction, GRP78 expression

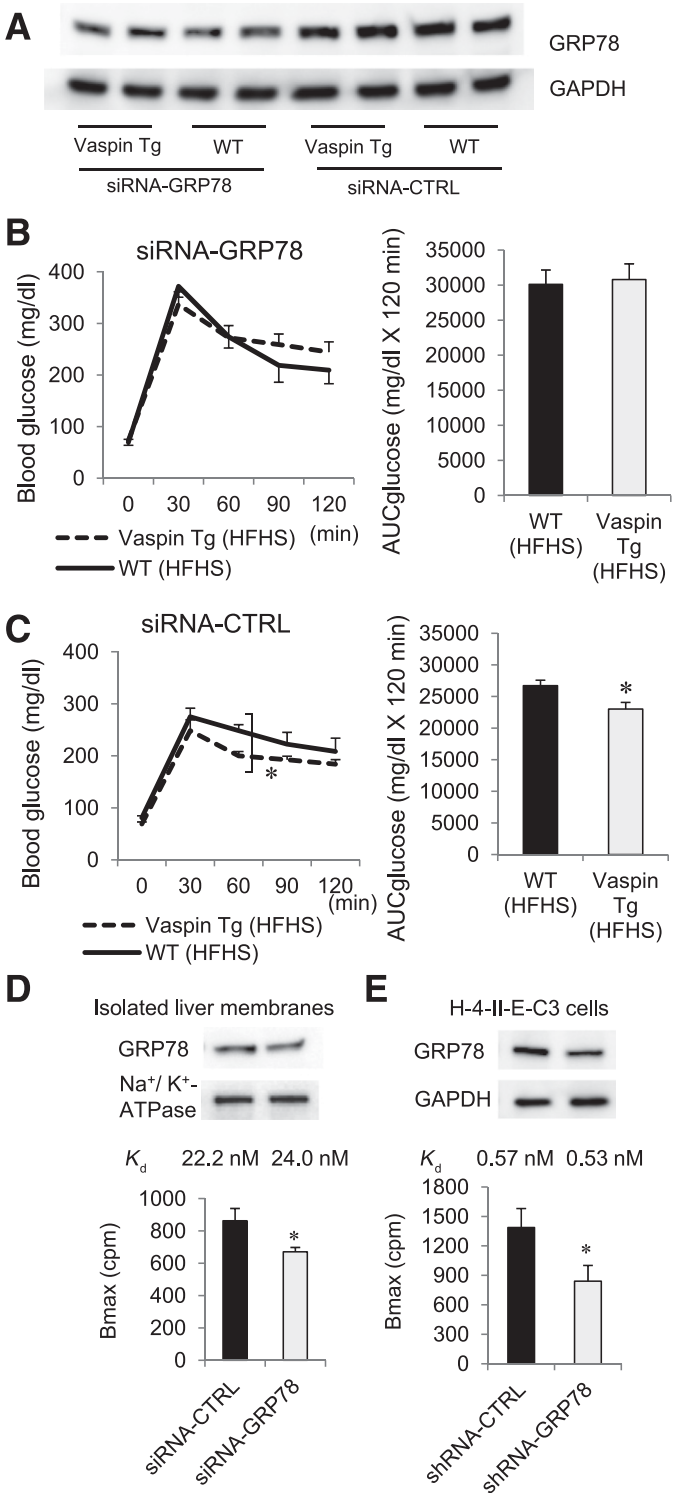

FIG. 5. Knockdown experiments by siRNA and shRNA lentivirus for GRP78. *A*: Glucose tolerance test in WT and vaspin Tg HFHS mice and siRNA-GRP78 (n = 3). With the treatment of siRNA-GRP78, beneficial effects in glucose tolerance in vaspin Tg mice were not observed. *B*: Glucose tolerance test in WT and vaspin Tg mice fed HFHS chow and treated with siRNA negative control (siRNA-CTRL) (n = 3). *P < 0.05 vs. WT HFHS mice treated with siRNA negative control. *C*: Western blot analyses of liver tissues. *D*: The binding activity of ^{125}I-vaspin using liver membrane fractions in vaspin Tg mice fed HFHS chow. Binding affinity of ^{125}I-vaspin was not altered by the treatment of siRNA-GRP78 by Scatchard analysis. B_{max} was reduced in the isolated liver membranes by the treatment of siRNA-GRP78. *P < 0.05 vs. siRNA negative control. *E*: Cell binding assay of ^{125}I-vaspin using cultured H-4-II-E-C3. B_{max} was reduced in H-4-II-E-C3 cells by the treatment of shRNA-GRP78 lentivirus. *P < 0.05 vs. shRNA negative control. K_d, dissociation constant.

inhibits the insulin- and ER stress–induced hepatic steatosis in *db/db* mice (6). Although GRP78 heterozygocity attenuates the diet-induced obesity and insulin resistance, Ye et al. (5) discuss the hypothesis that compensatory upregulation of GRP94 and protein disulfide isomerase, as well as other adaptive UPRs, is responsible for the therapeutic effects. Since the combination of GRP78 with ligands and associated anchor proteins exerts diverse biological consequences

such as cell survival and apoptosis, vaspin itself, anti-GRP78 antibodies, or GRP78-interacting small molecules mimicking beneficial action of vaspin need to be screened for the treatment of metabolic syndrome. In autoimmune diseases, anti-citrullinated protein antibodies, specific autoantibodies in rheumatoid arthritis, bind to GRP78 and enhance NF-κB activity and tumor necrosis factor-α production (28). Thus, anti-GRP78 antibodies and GRP78-interacting small molecules should be functionally tested as to whether they have antiapoptotic/proapoptotic potentials or anti-inflammatory/proinflammatory properties. α2M binds to cell-surface GRP78/MTJ-1, induces NF-κB activity, and activates phosphatidylinositol 3-kinase/Akt signal, which results in antiapoptosis, cell proliferation, and survival of tumor cells (21). Thus, the signals downstream of vaspin-GRP78/MTJ-1 pathways may induce NF-κB activity and production of proinflammatory cytokines in the setting of obesity and metabolic syndrome. In the current study, however, vaspin ameliorated ER stress and exerted anti-inflammatory actions in liver via vaspin-GRP78/MTJ-1 pathway (Fig. 6). Similar findings have been reported, i.e., that vaspin inhibits NF-κB activation and prevents tumor necrosis factor-α–induced expression of intracellular adhesion molecule-1 in vascular smooth muscle cells (29).

There are some limitations to the current investigation. Since the treatment with siRNA-GRP78 deteriorated glucose tolerance in both vaspin Tg and WT mice in the current study, the GRP78-induced beneficial effects in obesity were not completely dependent on the vaspin-mediated pathway; thus, targeting the GRP78 may be beneficial rather than using vaspin itself for the development of new therapeutic modalities. Another limitation is that direct biological actions of vaspin on adipose tissues were not clearly demonstrated in the study. GRP78 is also expressed in the adipocytes in vivo, and vaspin is >expressed in both intracellular and extracellular compartments. Vaspin may exert various biological effects on adipocytes such as reduction of adipocyte size and anti-inflammatory action by interacting with cell-surface GRP78 or ER-associated GRP78. Precise mechanisms of the direct action of vaspin on adipose tissues remain to be investigated in future studies. The last limitation is that where vaspin binds to the region of GRP78 is still uncharacterized. α2MG binds to the region at amino acids 98–115 (30) and competed with the binding of vaspin on GRP78. In addition, both anti-GRP78 *N*-20 and C-20 antibodies interfered with the binding of GRP78, vaspin binding, and the subsequent signaling events. It is still not clear whether α2MG and anti-GRP78 antibodies directly compete with vaspin or interfere with the vaspin binding by the alteration of conformation or function of GRP78 molecules.

Poor prognosis of the majority of tumors correlates with the expression of cell-surface GRP78 and presence of autoantibodies, which mediates prosurvival signals and responses to cellular stress. Thus, blocking anti-GRP78 antibodies, small molecule inhibitors, anti–cancer agent conjugated with vehicle targeted to GRP78, or GRP78 promoter–driven expression of suicide genes may be expected in the treatment of cancers (18). Vaspin indeed has a beneficial role in obesity in the metabolic dysfunctions, and the only concern to be addressed is whether vaspin promotes the tumor growth by acting on the cell-surface GRP78 on tumor cells. However, the lack of apparent carcinogenesis processes in vaspin Tg mice in our experiments negates the possibilities of development of neoplasm. Taken together, targeting GRP78 by vaspin or vaspin-mimicking antibodies or small molecules is beneficial for therapeutics for obesity and its related insulin resistance by ameliorating ER stress in the liver.

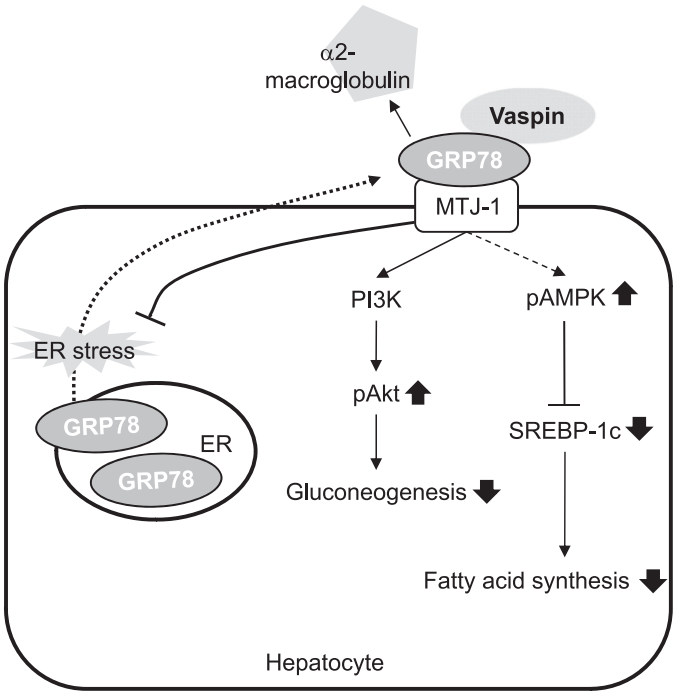

FIG. 6. Schematic drawing of the mechanism of vaspin action in hepatocytes.

ACKNOWLEDGMENTS

This research was supported by Grant-in-Aid for Young Scientists (B) (24790926) to A.N., Grant-in-Aid for Scientific Research (B) (23390241), Challenging Exploratory Research (23659470), Grant-in-Aid for Scientific Research on Innovative Areas ("Molecular Basis and Disorders of Control of Appetite and Fat Accumulation") (23126516) to J.W., and Grant-in-Aid for Scientific Research (A) (21249053) to H.M. from the Ministry of Education, Culture, Sports, Science and Technology of Japan.

K.Hig. is employed by Metabolome Pharmaceuticals, Inc. No other potential conflicts of interest relevant to this article were reported.

A.N. and J.W. designed and performed most of the experiments, conceived the study, and wrote the manuscript. I.I. designed and performed most of the experiments. K.Hig. performed Tg and knockout animal experiments and prepared rhVaspin. S.T., K.M., M.K., K.I., T.T., A.K., K.Hid., and J.E. performed Tg and knockout animal experiments. C.S.H. and D.O. performed immunohistochemistry. Y.M. and R.M. performed quantitative RT-PCR. S.K. and Y.I. derived and cultured mouse embryonic stem cells and performed blast cyst injection. H.M. conceived the study and wrote the manuscript. J.W. is the guarantor of this work and, as such, had full access to all the data in the study and takes responsibility for the integrity of the data and the accuracy of the data analysis.

The authors thank Yoko Saito and Dr. Noriko Yamamoto at Okayama University Graduate School of Medicine, Dentistry and Pharmaceutical Sciences for excellent technical assistance.

REFERENCES

1. Hotamisligil GS. Endoplasmic reticulum stress and the inflammatory basis of metabolic disease. Cell 2010;140:900–917
2. Ozcan U, Cao Q, Yilmaz E, et al. Endoplasmic reticulum stress links obesity, insulin action, and type 2 diabetes. Science 2004;306:457–461
3. Ozawa K, Miyazaki M, Matsuhisa M, et al. The endoplasmic reticulum chaperone improves insulin resistance in type 2 diabetes. Diabetes 2005; 54:657–663
4. Nakatani Y, Kaneto H, Kawamori D, et al. Involvement of endoplasmic reticulum stress in insulin resistance and diabetes. J Biol Chem 2005;280: 847–851
5. Ye R, Jung DY, Jun JY, et al. Grp78 heterozygosity promotes adaptive unfolded protein response and attenuates diet-induced obesity and insulin resistance. Diabetes 2010;59:6–16
6. Kammoun HL, Chabanon H, Hainault I, et al. GRP78 expression inhibits insulin and ER stress-induced SREBP-1c activation and reduces hepatic steatosis in mice. J Clin Invest 2009;119:1201–1215
7. Wada J. Vaspin: a novel serpin with insulin-sensitizing effects. Expert Opin Investig Drugs 2008;17:327–333
8. Hida K, Wada J, Eguchi J, et al. Visceral adipose tissue-derived serine protease inhibitor: a unique insulin-sensitizing adipocytokine in obesity. Proc Natl Acad Sci USA 2005;102:10610–10615
9. Blüher M. Vaspin in obesity and diabetes: pathophysiological and clinical significance. Endocrine 2012;41:176–182
10. Chang HM, Lee HJ, Park HS, et al. Effects of weight reduction on serum vaspin concentrations in obese subjects: modification by insulin resistance. Obesity (Silver Spring) 2010;18:2105–2110
11. Youn BS, Klöting N, Kratzsch J, et al. Serum vaspin concentrations in human obesity and type 2 diabetes. Diabetes 2008;57:372–377
12. Tan BK, Heutling D, Chen J, et al. Metformin decreases the adipokine vaspin in overweight women with polycystic ovary syndrome concomitant with improvement in insulin sensitivity and a decrease in insulin resistance. Diabetes 2008;57:1501–1507
13. Seeger J, Ziegelmeier M, Bachmann A, et al. Serum levels of the adipokine vaspin in relation to metabolic and renal parameters. J Clin Endocrinol Metab 2008;93:247–251
14. Hensley LL, Ranganathan G, Wagner EM, et al. Transgenic mice expressing lipoprotein lipase in adipose tissue. Absence of the proximal 3′-untranslated region causes translational upregulation. J Biol Chem 2003;278:32702–32709
15. Horai R, Asano M, Sudo K, et al. Production of mice deficient in genes for interleukin (IL)-1alpha, IL-1beta, IL-1alpha/beta, and IL-1 receptor antagonist shows that IL-1beta is crucial in turpentine-induced fever development and glucocorticoid secretion. J Exp Med 1998;187:1463–1475
16. Zhang Y, Wada J, Yasuhara A, et al. The role for HNF-1beta-targeted collectrin in maintenance of primary cilia and cell polarity in collecting duct cells. PLoS ONE 2007;2:e414
17. Yilmaz Y. Circulating vaspin and its relationship with insulin sensitivity, adiponectin and liver histology in subjects with non-alcoholic steatohepatitis. Scand J Gastroenterol 2012;47:489–490
18. Zhang LH, Zhang X. Roles of GRP78 in physiology and cancer. J Cell Biochem 2010;110:1299–1305
19. Sato M, Yao VJ, Arap W, Pasqualini R. GRP78 signaling hub a receptor for targeted tumor therapy. Adv Genet 2010;69:97–114
20. Gonzalez-Gronow M, Selim MA, Papalas J, Pizzo SV. GRP78: a multifunctional receptor on the cell surface. Antioxid Redox Signal 2009;11:2299–2306
21. Quinones QJ, de Ridder GG, Pizzo SV. GRP78: a chaperone with diverse roles beyond the endoplasmic reticulum. Histol Histopathol 2008;23:1409–1416
22. Misra UK, Pizzo SV. Modulation of the unfolded protein response in prostate cancer cells by antibody-directed against the carboxyl-terminal domain of GRP78. Apoptosis 2010;15:173–182
23. Misra UK, Sharma T, Pizzo SV. Ligation of cell surface-associated glucose-regulated protein 78 by receptor-recognized forms of alpha 2-macroglobulin: activation of p21-activated protein kinase-2-dependent signaling in murine peritoneal macrophages. J Immunol 2005;175:2525–2533
24. Misra UK, Gonzalez-Gronow M, Gawdi G, Pizzo SV. The role of MTJ-1 in cell surface translocation of GRP78, a receptor for alpha 2-macroglobulin-dependent signaling. J Immunol 2005;174:2092–2097
25. Misra UK, Deedwania R, Pizzo SV. Binding of activated alpha2-macroglobulin to its cell surface receptor GRP78 in 1-LN prostate cancer cells regulates PAK-2-dependent activation of LIMK. J Biol Chem 2005;280:26278–26286
26. Shani G, Fischer WH, Justice NJ, Kelber JA, Vale W, Gray PC. GRP78 and Cripto form a complex at the cell surface and collaborate to inhibit transforming growth factor beta signaling and enhance cell growth. Mol Cell Biol 2008;28:666–677
27. Philippova M, Ivanov D, Joshi MB, et al. Identification of proteins associating with glycosylphosphatidylinositol- anchored T-cadherin on the surface of vascular endothelial cells: role for Grp78/BiP in T-cadherin-dependent cell survival. Mol Cell Biol 2008;28:4004–4017
28. Lu MC, Lai NS, Yu HC, Huang HB, Hsieh SC, Yu CL. Anti-citrullinated protein antibodies bind surface-expressed citrullinated Grp78 on monocyte/macrophages and stimulate tumor necrosis factor alpha production. Arthritis Rheum 2010;62:1213–1223
29. Phalitakul S, Okada M, Hara Y, Yamawaki H. Vaspin prevents TNF-α-induced intracellular adhesion molecule-1 via inhibiting reactive oxygen species-dependent NF-κB and PKCθ activation in cultured rat vascular smooth muscle cells. Pharmacol Res 2011;64:493–500
30. Gonzalez-Gronow M, Cuchacovich M, Llanos C, Urzua C, Gawdi G, Pizzo SV. Prostate cancer cell proliferation in vitro is modulated by antibodies against glucose-regulated protein 78 isolated from patient serum. Cancer Res 2006;66:11424–11431